# Supporting Information

# MOF derived $ZnCo_2O_4$ porous hollow spheres functionalized with Ag nanoparticles for a long-cycle and high-capacity lithium ion battery anode

*Won-Tae Koo, Hye-Yeon Jang, Chanhoon Kim, Ji-Won Jung, Jun Young Cheong, and Il-Doo Kim**

Department of Materials Science and Engineering, Korea Advanced Institute of Science and Technology (KAIST), 291 Daehak-ro, Yuseong-gu, Daejeon 34141, Republic of Korea

*E-mail: idkim@kaist.ac.kr

**Table of Contents**

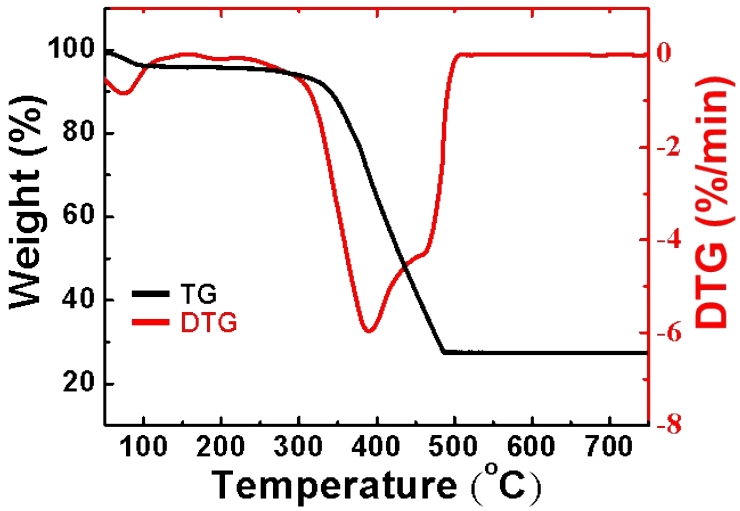


**Fig. S1** TG and DTG curves of BM-ZIF_PS in the temperature range of 50–750 °C under air atmosphere.

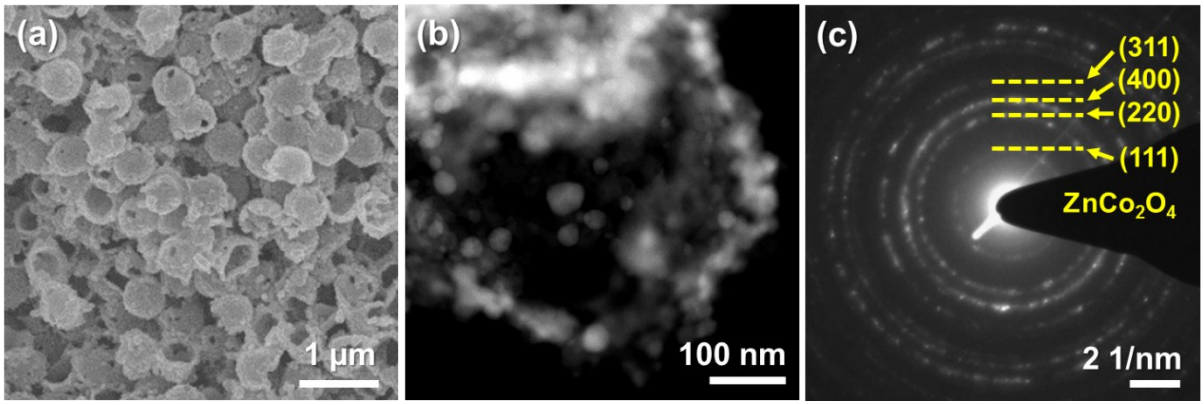


**Fig. S2** (a) SEM image of $ZnCo_2O_4$ HSs, (b) STEM image of $ZnCo_2O_4$@Ag HSs, and (c) SAED patterns of $ZnCo_2O_4$@Ag HSs.

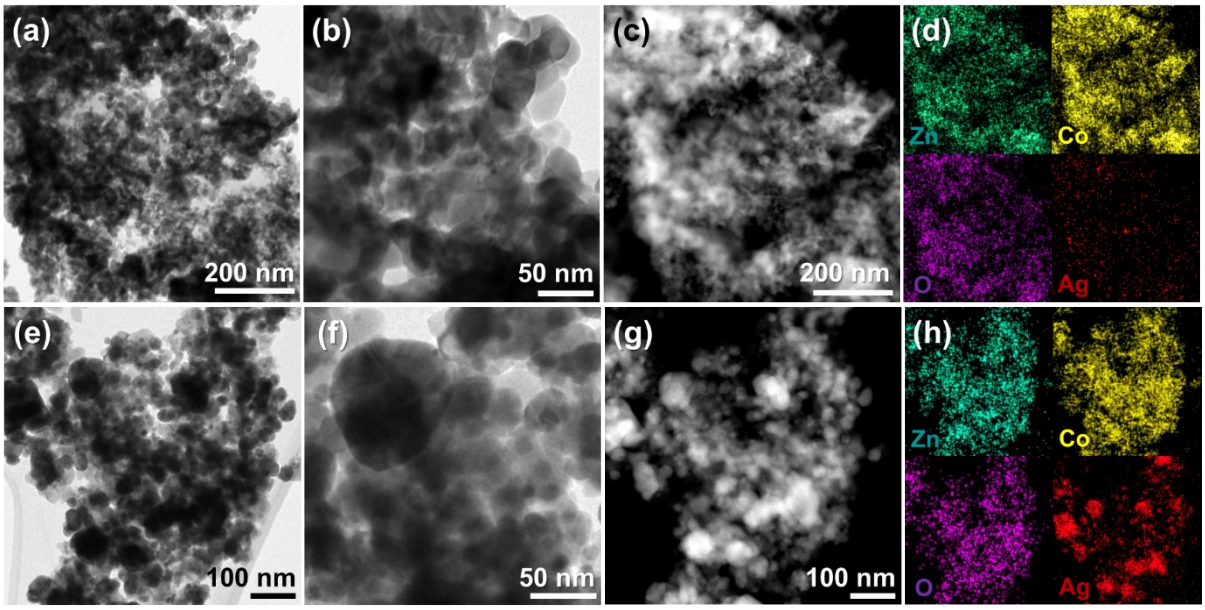


**Fig. S3** TEM analyses of $ZnCo_2O_4$@Ag HSs *via* Ag-mirror reaction using 1.7 mM (a-d) and 15 mM (e-h) of $AgNO_3$. TEM images (a,e), high magnification TEM images (b,f), STEM images (c,g), and EDS elemental mapping images (d,h).

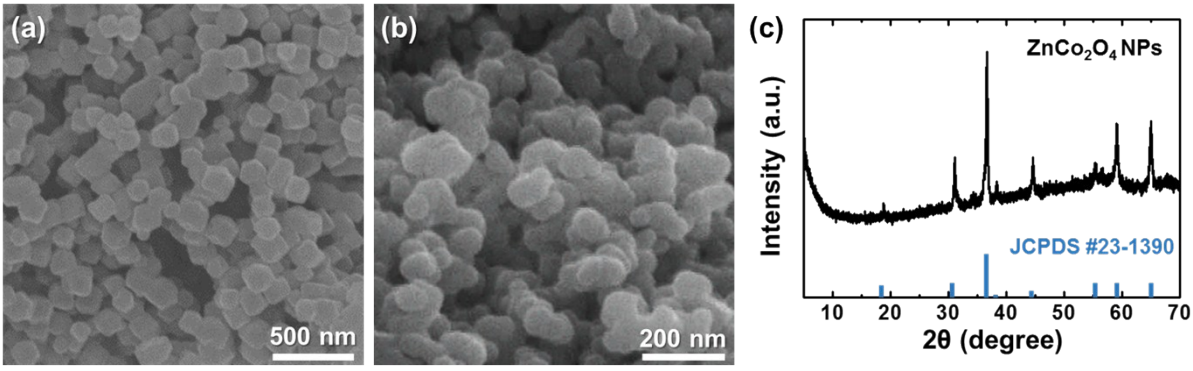


**Fig. S4** SEM images of (a) BM-ZIFs and (b) $ZnCo_2O_4$ NPs after calcination at 450 °C, and (c) XRD analysis of $ZnCo_2O_4$ NPs.

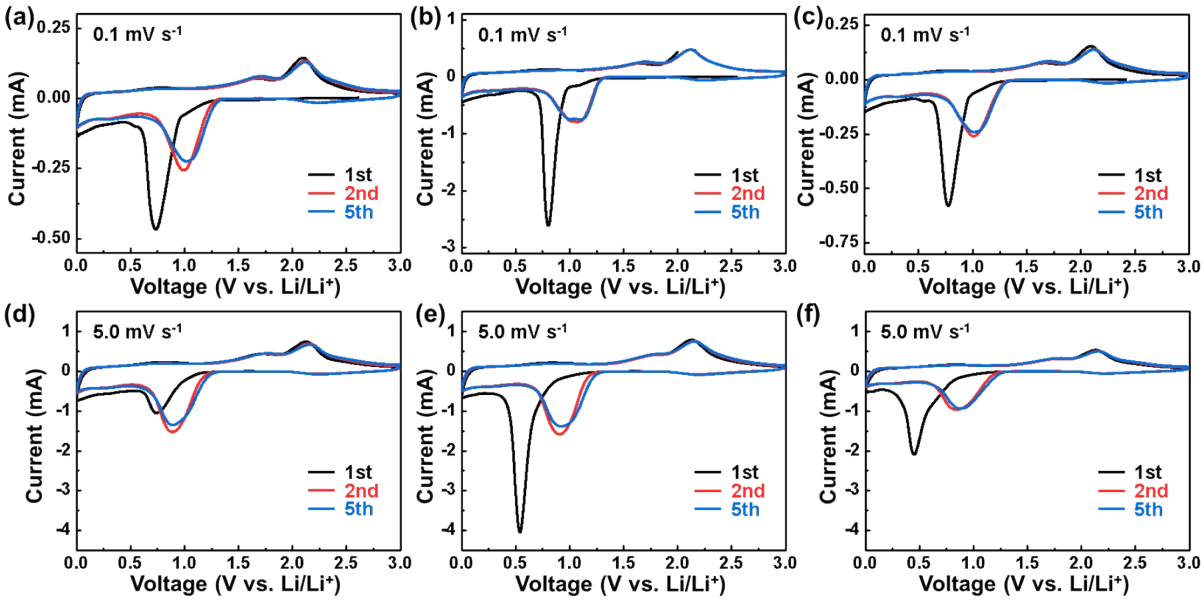


**Fig**. **S5** CV curves of 1st, 2nd, and 5th cycles at a scan rate of 0.1 mV $s^{-1}$ for (a) $ZnCo_2O_4$ NPs, (b) $ZnCo_2O_4$ HSs, and (c) $ZnCo_2O_4$@Ag HSs, respectively, with a voltage range of 0.01-3.0 V. CV curves of 1st, 2nd, and 5th cycles at a scan rate of 5.0 mV $s^{-1}$ for (d) $ZnCo_2O_4$ NPs, (e) $ZnCo_2O_4$ HSs, and (f) $ZnCo_2O_4$@Ag HSs.

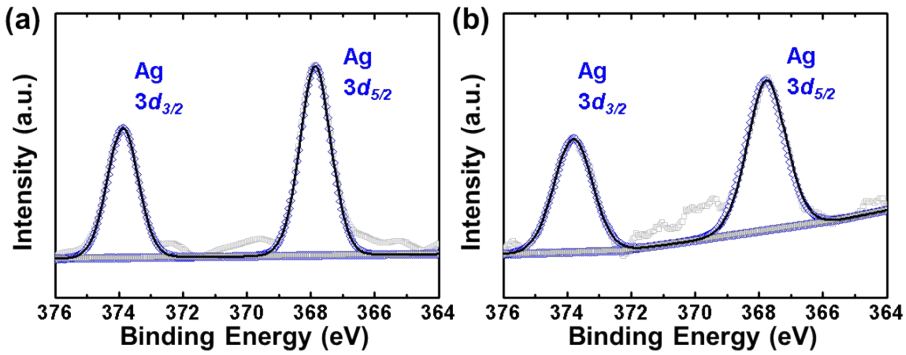


**Fig**. **S6** High-resolution XPS analysis spectrum of Ag 3*d* for $ZnCo_2O_4$@Ag HSs after 10 times of galvanostatic charging/discharging (a) with fully lithiated state, and (b) fully delithiated state.

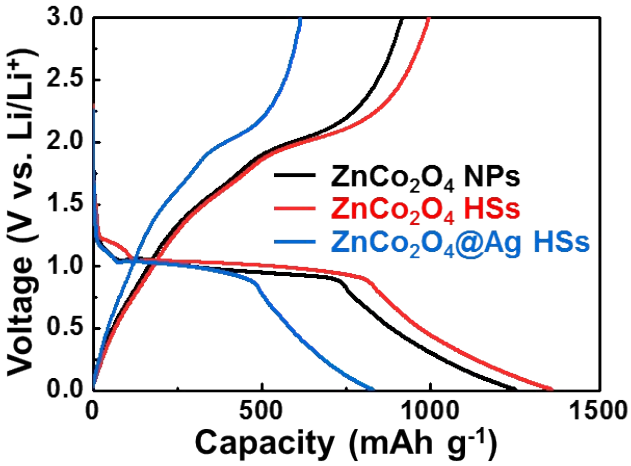


**Fig**. **S7** The first galvanostatic cycle discharge/charge voltage profiles for $ZnCo_2O_4$ NPs, $ZnCo_2O_4$ HSs, and $ZnCo_2O_4$@Ag HSs at a current density of 1 A $g^{-1}$.

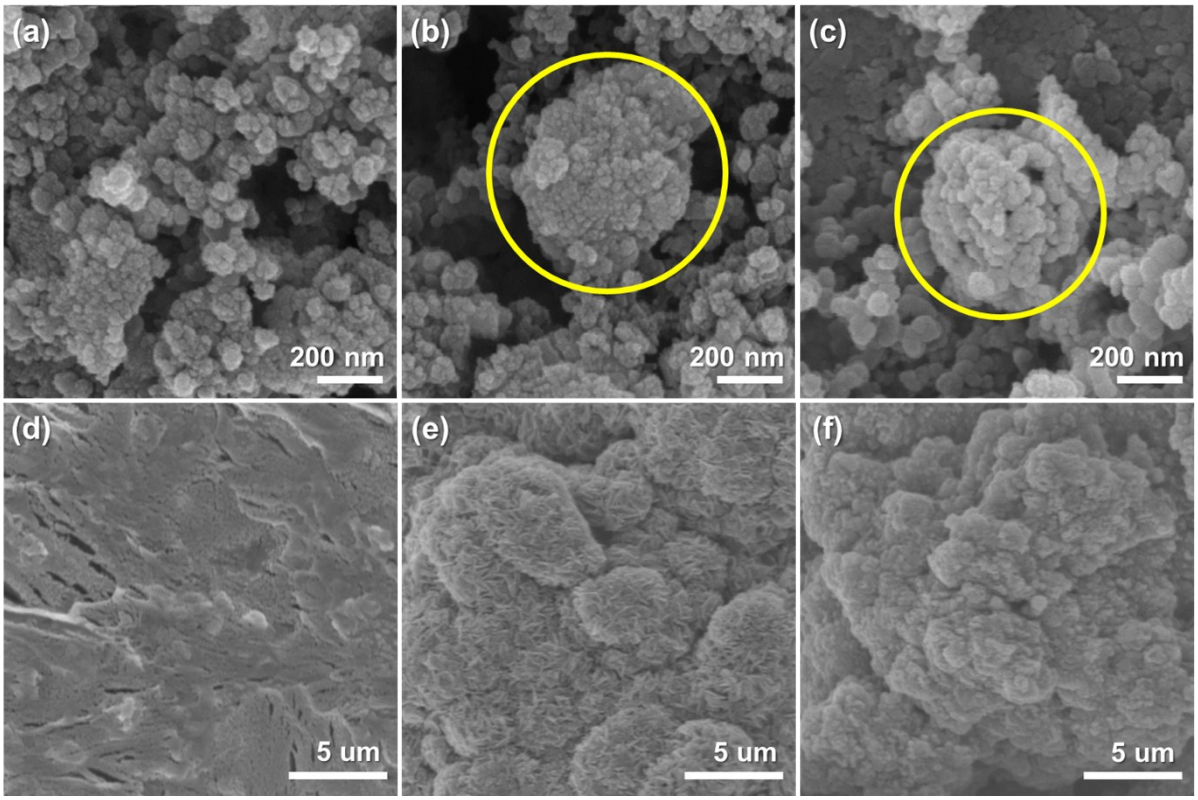


**Fig**. **S8** SEM images of the surface of (a) $ZnCo_2O_4$ NPs, (b) $ZnCo_2O_4$ HSs, and (c) $ZnCo_2O_4$@Ag HSs electrodes before cycling. *Ex-situ* SEM images of fully delithiated (d) $ZnCo_2O_4$ NPs, (e) $ZnCo_2O_4$ HSs, and (f) $ZnCo_2O_4$@Ag HSs electrodes after 200 cycles.

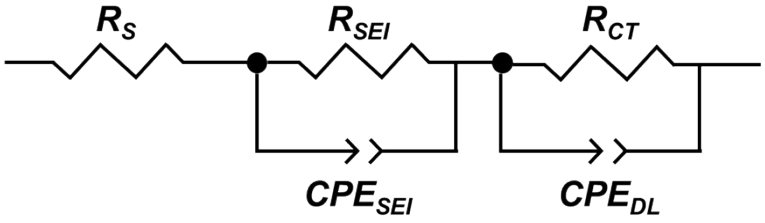


**Fig**. **S9** Equivalent circuit model for $ZnCo_2O_4$ NPs, $ZnCo_2O_4$ HSs, and $ZnCo_2O_4$@Ag HSs electrodes after cycling.

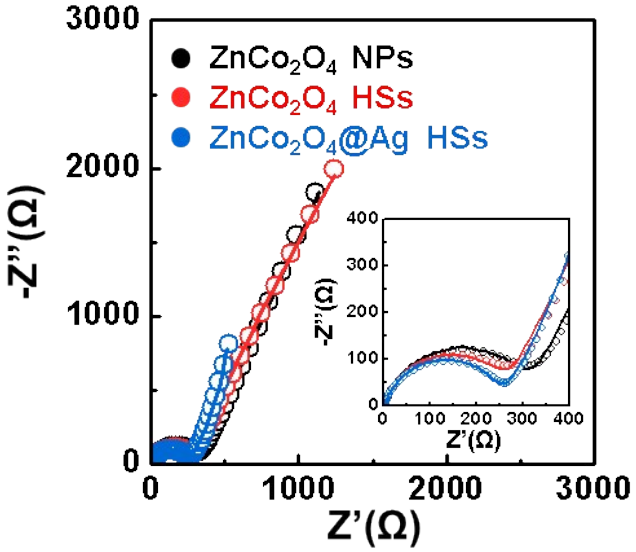


**Fig**. **S10** Nyquist plots of the fully delithiated $ZnCo_2O_4$ NPs, $ZnCo_2O_4$ HSs, and $ZnCo_2O_4$@Ag HSs before cycling.

**Table S1**. Capacity values of $ZnCo_2O_4$ NPs, $ZnCo_2O_4$ HSs, and $ZnCo_2O_4$@Ag HSs at high current densities of 10 A $g^{-1}$, 15 A $g^{-1}$, 20 A $g^{-1}$, and 0.5 A $g^{-1}$.

| | **10 A $g^{-1}$** | **15 A $g^{-1}$** | **20 A $g^{-1}$** | **0.5 A $g^{-1}$** |
|---|---|---|---|---|
| **$ZnCo_2O_4$ NPs** | 562 mAh $g^{-1}$ | 454 mAh $g^{-1}$ | 355 mAh $g^{-1}$ | 784 mAh $g^{-1}$ |
| **$ZnCo_2O_4$ HSs** | 583 mAh $g^{-1}$ | 479 mAh $g^{-1}$ | 384 mAh $g^{-1}$ | 780 mAh $g^{-1}$ |
| **$ZnCo_2O_4$@Ag HSs** | 627 mAh $g^{-1}$ | 610 mAh $g^{-1}$ | 572 mAh $g^{-1}$ | 689 mAh $g^{-1}$ |

**Table S2.** Cycling performance and rate capabilities of representative $ZnCo_2O_4$ anode materials for Li-ion batteries.

| Active material | Cycling performance | Rate capability | Reference |
|---|---|---|---|
| Mesoporous $ZnCo_2O_4$ microspheres | 721 mAh $g^{-1}$ after 80 cycles at 0.1 A $g^{-1}$ | 382 mAh $g^{-1}$ at 5.0 A $g^{-1}$ | 1 |
| Porous spinel $Zn_xCo_{3-x}O_4$ hollow polyhedra | 990 mAh $g^{-1}$ after 50 cycles at 0.1 A $g^{-1}$ | 575 mAh $g^{-1}$ at 9.0 A $g^{-1}$ | 2 |
| ZnO/$ZnCo_2O_4$/C core/shell | 669 mAh $g^{-1}$ after 250 cycles at 0.5 A $g^{-1}$ | 715 mAh $g^{-1}$ at 1.6 A $g^{-1}$ | 3 |
| Te@$ZnCo_2O_4$ nanofibers | 956 mAh $g^{-1}$ after 100 cycles at 0.1 A $g^{-1}$ | 587 mAh $g^{-1}$ at 1.0 A $g^{-1}$ | 4 |
| $ZnCo_2O_4$ 3D hierarchical twin microspheres | 550 mAh $g^{-1}$ after 2000 cycles at 5.0 A $g^{-1}$ | 790 mAh $g^{-1}$ at 10 A $g^{-1}$ | 5 |
| $ZnCo_2O_4$@Ag HSs | 616 mAh $g^{-1}$ after 900 cycles at 1.0 A $g^{-1}$ | 572 mAh $g^{-1}$ at 20 A $g^{-1}$ | In this work |

**Table S3.** Fitted electrochemical impedance component values of $ZnCo_2O_4$ NPs, $ZnCo_2O_4$ HSs, and $ZnCo_2O_4$@Ag HSs electrodes after (a) 1 cycle and (b) 200 cycles.

| **(a)** | **$R_{SEI}$ (Ω)** | **$R_{CT}$ (Ω)** |
|---|---|---|
| **$ZnCo_2O_4$ NPs** | 1.64 | 17.1 |
| **$ZnCo_2O_4$ HSs** | 1.62 | 19.6 |
| **$ZnCo_2O_4$@Ag HSs** | 1.82 | 65.2 |

| **(b)** | **$R_{SEI}$ (Ω)** | **$R_{CT}$ (Ω)** |
|---|---|---|
| **$ZnCo_2O_4$ NPs** | 4.58 | 45.9 |
| **$ZnCo_2O_4$ HSs** | 3.38 | 21.1 |
| **$ZnCo_2O_4$@Ag HSs** | 2.74 | 18.1 |

**References**

[1] L. Hu, B. Qu, C. Li, Y. Chen, L. Mei, D. Lei, L. Chen, Q. Li and T. Wang, *J. Mater. Chem. A,* 2013, **1**, 5596–5602.

[2] R. Wu, X. Qian, K. Zhou, J. Wei, J. Lou and P. M. Ajayan, *ACS Nano*, 2014, **8**, 6297–6303.

[3] X. Ge, Z. Li, C. Wang and L. Yin, *ACS Appl. Mater. Interfaces*, 2015, **7**, 26633–26642.

[4] G. Huang, Q. Li, D. Yin and L. Wang, *Adv. Funct. Mater.*, 2017, **27**, 1604941.

[5] J. Bai, X. Li, G. Liu, Y. Qian and S. Xiong, *Adv. Funct. Mater.*, 2014, **24**, 3012–3020.